LBL-10946 c.2
Preprint

Lawrence Berkeley Laboratory
UNIVERSITY OF CALIFORNIA

Materials & Molecular Research Division

Submitted to the Journal of Materials Science

SLOW DEGRADATION AND ELECTRON INJECTION IN SODIUM-β ALUMINAS

Lutgard C. De Jonghe, Leslie Feldman, and Andrew Buechele

May 1980

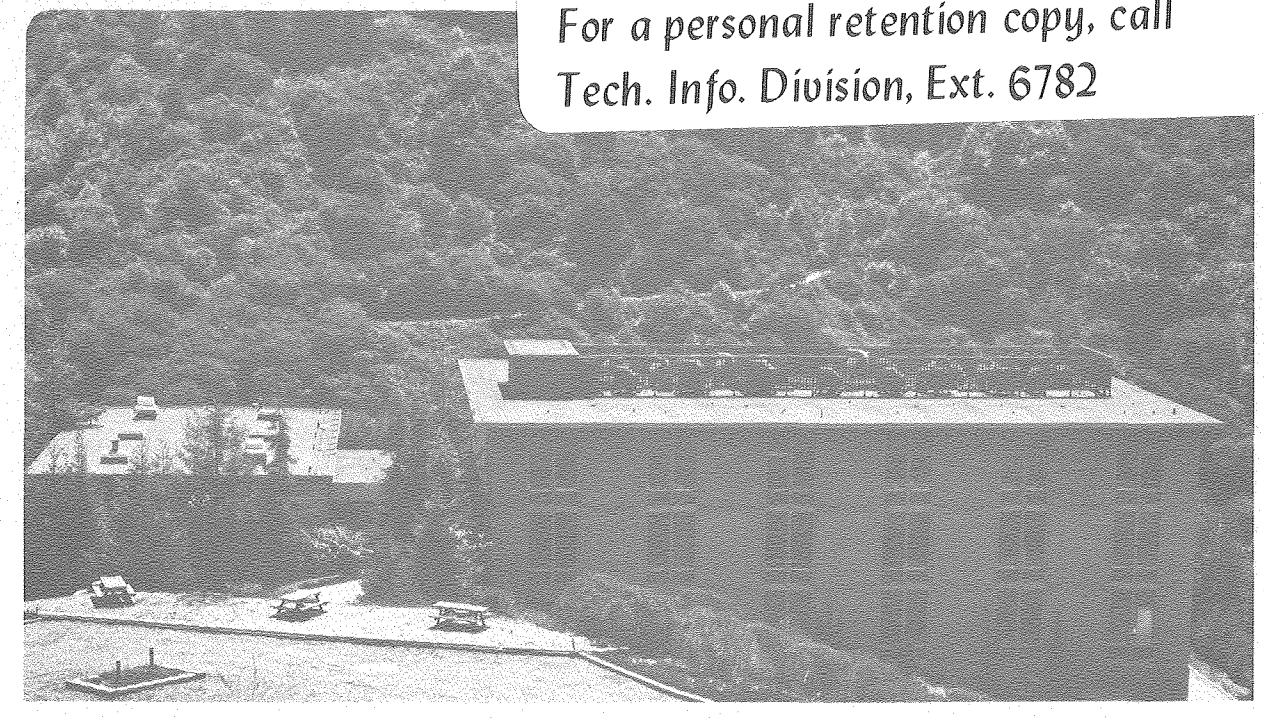

Prepared for the U.S. Department of Energy under Contract W-7405-ENG-48

DISCLAIMER

SLOW DEGRADATION AND ELECTRON INJECTION IN SODIUM-β ALUMINAS

Lutgard C. De Jonghe, Leslie Feldman, and Andrew Buechele

Materials and Molecular Research Division
Lawrence Berkeley Laboratory
and
Department of Materials Science and Mineral Engineering
University of California
Berkeley, California 94720

ABSTRACT

Slow degradation was observed in sodium-beta alumina electrolyte subjected to long term in cycling Na/S cells. The degradation propagated as a layer from the sodium side. It involved the internal deposition of sodium metal during current passage. This Mode II degradation was distinct from chemical coloration and from the Mode I failure (Poiseuille pressure due to cathodic deposition driving isolated cracks). Degradation was also observed on the sulfur side of the electrolyte, and was associated with the graphite felt "imprinting effect." Plausible mechanisms are proposed for the observed effects. It is thought that the Mode II degradation resulted from electron injection into the solid electrolyte from the beta alumina/sodium metal interface during the charging cycle.

I. Introduction

Sodium-beta aluminas used as solid electrolytes in sodium-sulfur batteries degrade during cell cycling. The type of degradation reported frequently to date was first discussed by Armstrong et al.[1], and has been examined in more detail by a number of authors [2-10]. This degradation, called Mode I here, involves the propagation of a sodium-filled crack driven by a cathodic deposition mechanism. In general, a significant threshold current density needs to be exceeded before the rapid Mode I fracture-degradation is initiated.

From our examinations of a number of sodium-beta alumina electrolytes that were used in Na/S cells, it appeared that a second type of degradation was active. This mode of degradation, called Mode II here, manifests itself as a damage layer developing from the sodium side of the electrolyte. Degradation was also found to develop from the sulfur side of the electrolyte. Additionally, the usual chemical coloration propagating from the sodium electrode was also present. In this paper we first comment on the Mode I rapid breakdown and on the chemical coloration, and then discuss our observations on the Mode II progressive degradation.

II. Experimental

The used electrolytes were obtained from the General Electric Research and Development Center. They were beta alumina electrolytes with a composition of 9.6 wt % Na_2O, 0.25 wt %

Li_2O, balance Al_2O_3. The starting material was a commercial sodium-beta alumina containing approximately 7.5 wt % Na_2O, with about 0.15 wt % SiO_2 as the major impurity (Alcoa-XB-2 "Superground," Aluminum Company of America, Pittsburgh, Pennsylvania). The electrolytes had been cycled in sodium/sulfur cells at current densities of approximately 100 mA . cm^{-2}. The cells operated around 300°C into the two-phase region of the sodium polysulfide electrode. After cycling, the cells were cleaned with methanol and stored prior to examination in our laboratory. During storage, the cells had been exposed to atmosphere for a period of about one week.

The surfaces of as-received electrolytes and of sectioned and polished electrolytes were examined with optical microscopy. It was necessary to use the staining methods described earlier by De Jonghe et al. [12] to reveal the flaws. The staining was carried out in a one-molar aqueous solution of silver nitrate at a temperature of about 80°C for between one-half and one hour. Comparisons of the electrolytes show that this staining procedure did not introduce any additional flaws that could be detected with optical microscopy. The stained electrolytes were examined using polarized light to reduce the surface scattering. Additional observations on unstained electrolytes were performed with scanning microscopy, high-voltage transmission electron microscopy, and analytical transmission electron microscopy.

III. Results and Discussions

3.1. Mode I Breakdown: Rapid-Crack Propagation.

In the Mode I failure, a single sodium-filled crack is propagated through the electrolyte. Once a critical flaw has been formed, propagation is rapid. The stresses arise from the Poiseuille pressure gradient generated by the flow of the sodium out of the crack. A number of difficulties remain for adequately predicting the macroscopic current densities at which the stress intensity at the sodium-filled crack tip exceeds K_{1C}, the critical stress intensity factor. Two classes of problems cause this difficulty: uncertainties in the boundary conditions, and anisotropic microstructures.

The exact calculation of the local cathodic deposition rates along the crack tip and faces is a complex problem. A first approach is the solution of the Laplacian for a particular crack geometry in a perfectly isotropic dielectric. This yields the primary current distribution. However, the situation becomes more complicated when the flaw is actually carrying current. The Poiseuille pressures that are generated will generate a counter-EMF, ΔE, at the interfaces of a magnitude $\Delta E = -V_o P/F$, where V_o = the molar volume of Na, P is the local pressure at the crack face, and F is Faraday's constant. This problem has been discussed in some detail by Brennan [11]. Brennan also discussed the importance of the electrolyte-electrode interface charge-transfer resistance on

the critical current densities. These overvoltages can be significant in crack areas where large local pressures or large local current densities are calculated. The generated overvoltages act to decrease the effects of current focusing on the crack tip. Brennan's analysis yields a good approximation of the secondary current distribution for the ideal crack. The problem is analogous to that of dendrite growth during cathodic plating and to other electro-deposition problems such as the ones discussed by Kasper. The same considerations should be of significance in the calculation of electrode current inhomogeneities such as those recently reported by Virkar et al. [18]. The present problems in the details of the current distribution on the crack faces then show up as uncertainties in the pressure distribution on the crack faces, and hence as uncertainties in K_1 at the crack tip.

The anisotropy of sodium-beta alumina microstructures is perhaps an even more serious problem. It is precisely in the initiation stage, when the critical flaws are on the order of the grain size, that microstructural anisotropy is most influential. The local microstructure will strongly affect the way in which the crack is fed. We have considered the geometries that are most effective in feeding sodium-filled cracks on the order of the grain size. It appears that grain boundaries can play an important role in the Mode I failure initiation, on the basis of local geometry alone [19].

3.2. Chemical Coloration.

It has been observed by various workers that sodium-beta alumina darkens significantly when in prolonged static contact with sodium metal at temperatures above the melting point of the sodium. This chemical darkening also proceeds in a layer-like fashion from the sodium/electrolyte interface without any current passage [20]. The chemical coloration can be enhanced very strongly if the sodium in the discolored electrolyte is exchanged for silver by immersing it in molten silver nitrate. This discoloration was also present in the examined electrolytes discussed here. The layer grows, however, far more rapidly than the Mode II degradation layer described below. At 300°C it has proceeded about 0.5 mm into the electrolyte after immersion in molten sodium for approximately 10 days. Transmission electron microscopy of the discolored regions has failed to reveal any imperfections that could be attributed to the chemical darkening. This indicates that the chemical darkening is due to point defects rather than to second-phase precipitation. Preliminary experiments in this laboratory have indicated that the coloring is associated with penetration of Na^+ into the spinel blocks. We will report the details of the experiments on chemical coloration by metallic sodium shortly.

3.3. Mode II Breakdown: Slow degradation

3.3.1. Sodium Side. Stained sodium/electrolyte interfaces of four cells are compared in Fig. 1 after a total charge transfer (charge + discharge) ranging from 23 to 703 A hrs. cm^{-2}. A

progressive though uneven darkening is observed. These surfaces were more closely examined with the optical microscopy (Fig. 2), but did not reveal any resolvable features of significance. Scanning electron microscopy of unstained sodium/electrolyte interfaces showed the formation of significant amounts of sodium carbonates (Fig. 3). Such carbonates can form when sodium-beta aluminas are exposed to moisture-containing atmosphere: NaOH that is formed on the surface scavenges the CO_2 in the air. It is interesting to note that the carbonate formation on the as-received samples that were exposed to atmosphere was significantly more extensive on those electrolytes that had been cycled longer. This suggested that the longer-cycled electrolytes might have contained more sodium, in agreement with the findings reported below. A more important observation is shown in Fig. 4. In these polished and stained cross-sections it is clearly shown that significant electrolyte damage has occurred in a layer-like fashion from the sodium/electrolyte interface. At 703 A hrs cm^{-2} this layer of degradation has progressed through about one-third of the tube wall. The white, spotty reflections were found to be subsurface from their focusing behavior in the optical microscope. We propose that they are microfractures caused by internal sodium deposition. Evidence supporting this description of this mode of degradation is presented in Figs. 5 and 6. Figure 5a is a high-voltage

transmission electron micrograph of a thick foil prepared by ion milling from the degraded region of an electrolyte subjected to 332 A hrs. cm^{-2} of charge transfer. The arrows indicate where sodium metal appears to have deposited. The deposition occurred at some grain boundaries, as well as at some grain triple junctions. Interestingly, analytical scanning transmission electron microscopy on degraded regions such as this showed that the degraded triple junctions contained silicon as well (Fig. 5b). It therefore appears that grain boundaries, as well as intergranular phases, are active in the Mode II degradation. Figure 6 shows a microfracture area, where excess sodium as well as silicon was detected with the analytical scanning transmission electron microscope. Some of the sodium in tin foils like these may have been lost to the atmosphere during foil preparation.

This slow Mode II sodium penetration cannot be accounted for by Poiseuille pressure arguments. Indeed, Mode I degradation leads invariably to rapid crack propagation. Instead, we propose that it involves electron injection from the sodium/beta alumina interface, followed by electron-Na^{+} recombination in the electrolyte. This type of recombination process could indeed lead to internal sodium deposition, generating sufficient stresses to cause local microfracture. The injection of electrons into beta-alumina could be greatly affected by a number of factors:

impurity and electronic surface states, the presence of other electron traps, and geometric field enhancements around sharply pointed sodium-filled flaws. Current injection from metal/insulator contacts has been treated extensively in the semiconductor literature (see, for example, Mark and Lampert [21]). As an example, when dealing with a space charge-limited current injection into a trap-free, perfect electronic insulator, an electronic current proportional to V^2/L^3 would be injected, where V is the applied voltage difference across the slab of insulator of thickness L. The actual current/voltage characteristics of the sodium/beta alumina contact are at present unknown. In general, however, it should be expected that the electron injection current would be proportional to V^n, where V is the voltage difference between the positive and negative electrolyte surfaces, and where $n > 1$. Such a voltage dependence on the electron injection current density might provide a plausible explanation for the observation that electrolytes cycled in sodium/sodium cells last considerably longer than those cycled in sodium/sulfur cells: The voltage difference across the electrolyte in sodium/sulfur cells is considerably larger than that in sodium/sodium cells for the same current density.

Mode I flaws were also observed in cycled electrolytes. An example is shown in Fig. 7. It could not be determined at which point of the cycling life this Mode I crack had formed. It is possible that the microcracking associated with the Mode II failure

might actually have initiated the Mode I failure. It is interesting to note that the Mode I crack shown in Fig. 7 did not remain perpendicular to the tube walls. We attribute this deflection to a basic instability in the Mode I geometry: A deflected crack is more effectively current-fed. This deflection can clearly lead to spalling of the electrolyte surfaces. Similar crack deflections have been observed by us in accelerated sodium/sodium testing of electrolyte tubes at 300°C [22].

3.3.2. Sulfur Side. Degradation was observed on the sulfur side of the used electrolytes as well. A macrograph comparing the four examined electrolytes is shown in Fig. 8. At short cycling times, the sulfur/electrolyte surface is virtually unaffected. At long cycling times a significant degradation occurs, as shown in Figs. 9a and 9b. Figure 9a clearly shows the "imprinting effect" that has been reported by other workers as well [23]. The light and dark regions in the electrolyte surface reflect the macrostructure of the graphite filler that was used to facilitate current extraction from the positive sulfur electrode. The decoration of these surfaces, with the method described earlier, revealed the presence of surface cracks (Fig. 9b). A cross-section of the electrolyte at the positive electrode is shown in Fig. 10. Again, a band of degradation is observed after extensive charge transfer. This layer appears quite nonuniform at low-charge transfer, but it is fully established after 703 A hrs cm^{-2}. At

present, this degradation has been less well-examined. Work on it is continuing. The indications are that again a sodium deposition has occurred. This highly unusual situation would require the positive interface to act as a pseudo-cathode during part of the charge of discharge cycle. We postulate that such a circumstance might arise during charging when a significant chemical polarization layer had developed in the sulfur electrode during the previous discharge cycle. Upon charging, then, this chemical polarization layer containing solid polysulfide phases would itself act as an electrolyte, causing the electrolyte surface to be at a cathodic potential with respect to the graphite fibers. Electrons arriving from the sodium side of the electrolyte, where electron injection occurred during charging, may then recombine with the sodium causing a mechanism of degradation to occur at the pseudo-cathode analogous to that of the negative electrolyte surface. We are currently investigating further the validity of this postulate.

IV. Conclusions

A second mode of degradation has been observed in sodium beta alumina solid electrolytes cycled in sodium/sulfur cells. This Mode II degradation propagates as a damage layer from the sodium/electrolyte interface. It is distinguished from the Mode I failure, which consists of isolated cracks propagating from the sodium side, and from the chemical discoloration. The Mode II

degradation appears to involve grain boundaries, as well as intergranular phases. The observations led to the postulates that the slow degradation could be attributed to electron injection and recombination during the charging cycle of the sodium/sulfur cell.

Degradation also developed on the sulfur side of the electrolyte. It has been postulated that a pseudo-cathode process occurs, also leading to sodium formation and penetration from the positive electrode.

V. Acknowledgments

Dr. S. Mitoff of the General Electric Research and Development Center, Schenectady, New York, is thanked for providing us with the used electrolytes.

This work was supported by the Electric Power Research Institute through their Division of Material Sciences, Office of Basic Energy Sciences, U.S. Department of Energy, under Contract No. W-7405-Eng-48.

VI. References

1. R.D. Armstrong, T. Dickinson, and J. Turner, Electrochim. Acta, 19 (1974) 187.
2. G.J. Tennenhouse, R.L. Ku, R.H. Richman, and T.J. Whalen, Bull. Amer. Ceram. Soc., 54 (1975) 523.
3. R.H. Richman and G.J. Tennenhous, J. Amer. Ceram. Soc., 58 (1975) 63.
4. D.K. Shetty, A.V. Virkar, and R.S. Gordon, in "Fracture Mechanics of Ceramics," Vol.4 (R.L. Bradt and D.P.H. Hasselman, Eds.), Plenum Press, New York, 1978, pp. 651-665.
5. R.W. Davidge, G. Tappin, J.R. McLaren, and G.J. May, J. Amer. Ceram. Soc., 58 (1979) 771.
6. C.A. Worrell and B.A.W. Redfern, J. Mat. Sci., 13 (1978) 1515.
7. R. Knodler and W. Bankal, J. Power Sources, 3 (1978) 23.
8. N.K. Gupta and G.J. Tennenhouse, J. Electrochem. Soc., 126 (1979) 145.
9. L.C. De Jonghe, L. Feldman, and P. Millett, Mat. Res. Bull., 14 (1979) 589.
10. I. Yasui and R.H. Doremus, J. Electrochem. Soc., 125 (1978) 1007.
11. M.P.J. Brennan, Electrochem. Acta, in press (1980).
12. L.C. De Jonghe and L. Feldman, Mat. Res. Bull., 15 (1980) 777.

13. C. Kasper, Trans. Electrochem. Soc., 77 (1940) 353, 365; 78 (1940) 131, 147; 82 (1942) 153.

14. C. Wagner, J. Electrochem. Soc., 98 (1951) 116.

15. J.L. Barton and J.O'M. Bockris, Proc. Royal Soc., London A268 (1962) 485.

16. A.R. Despic, J. Diggle, and J.O'M. Bockris, J. Electrochem. Soc. 116 (2969), 1503.

18. A.V. Virkar, L. Viswanathan, and D.R. Biswas, J. Mat. Sci. 15 (1980) 302.

19. For example, N. Weber and G. Tennenhouse, unpublished work.

20. N. Weber, T. Cole, and T.K. Hunt. Bull. Amer. Ceram. Soc., 59 (1980) 377. (Abstract 7-E-80)

21. M. Lampert and P. Mark, "Current Injection in Solids," Academic Press, New York, 1970, pp. 15ff.

22. A. Buechele and L.C. De Jonghe, unpublished work (1980).

23. "Research in Electrodes and Electrolytes for the Ford Sodium-Sulfur Battery," Research Staff, Ford Motor Company, Dearborn, Michigan 48121, January 1977.

Figure Captions

Fig. 1. Silver-stained electrolytes after a total charge transfer (charge + discharge) of 23, 271, 332, and 703 A hrs cm^{-2}. XBB 804 4133

Fig. 2. Silver-stained surface of electrolyte after 703 a hrs cm^{-2} of charge transfer, Na side. No significant features are observed. XBB 804 4123

Fig. 3. Sodium carbonates formed on Na side surface of electrolytes subjected to 703 and 23 A hrs cm^{-2} of charge transfer. Significantly more carbonates form on the electrolyte cycled longest. XBB 804 4134

Fig. 4. Damage layer progressing from the Na side of the electrolyte after charge transfer of 332 and 703 a hrs cm^{-2}. For the lower cycle life, the damage layer is uneven. XBB 804 4119

Fig. 5a. Sodium deposits in damage layer of electrolyte after charge transfer of 332 A hrs cm^{-2}. The sodium deposits are indicated with arrows. Both grain boundaries and grain triple junctions appear involved. Thick foil observed in high-voltage transmission electron microscope to minimize loss of Na. XBB 803 3889

Fig. 5b. Analytical microscopy shows that Si is present in the triple grain junction, where extra Na has deposited. CBB 803 3568

Fig. 6. Thick foil prepared from damage region of electrolyte subjected to 703 A hrs cm^{-2} of charge transfer. Microcracks associated with sodium deposition are arrowed. Care needs to be exercised to distinguish these cracks from cracks introduced in foil preparation. Thick foils are necessary for avoiding interference from foil artifacts. XBB 806 7055

Fig. 7. Mode I flaw, arrowed, in electrolyte after 703 A hrs cm^{-2} of charge transfer. These flaws, when present, always emanate from the Na side. XBB 804 4120

Fig. 8. Comparison of the four electrolytes after staining; sulfur sides after indicated charge transfers. XBB 804 4114

Fig. 9a. "Imprinting" effect of graphite fiber filler on S side of electrolyte. XBB 804 4125

Fig. 9b. The silver staining shows surface cracks associated with this imprinting. Electrolyte subjected to charge transfer of 703 A hrs cm^{-2}. XBB 804 4126

Fig. 10 Degradation of sulfur side of electrolyte after 332 and 703 A hrs cm^{-2}, after silver staining. The degradation layer becomes more uniform after prolonged electrolysis. XBB 804 4128

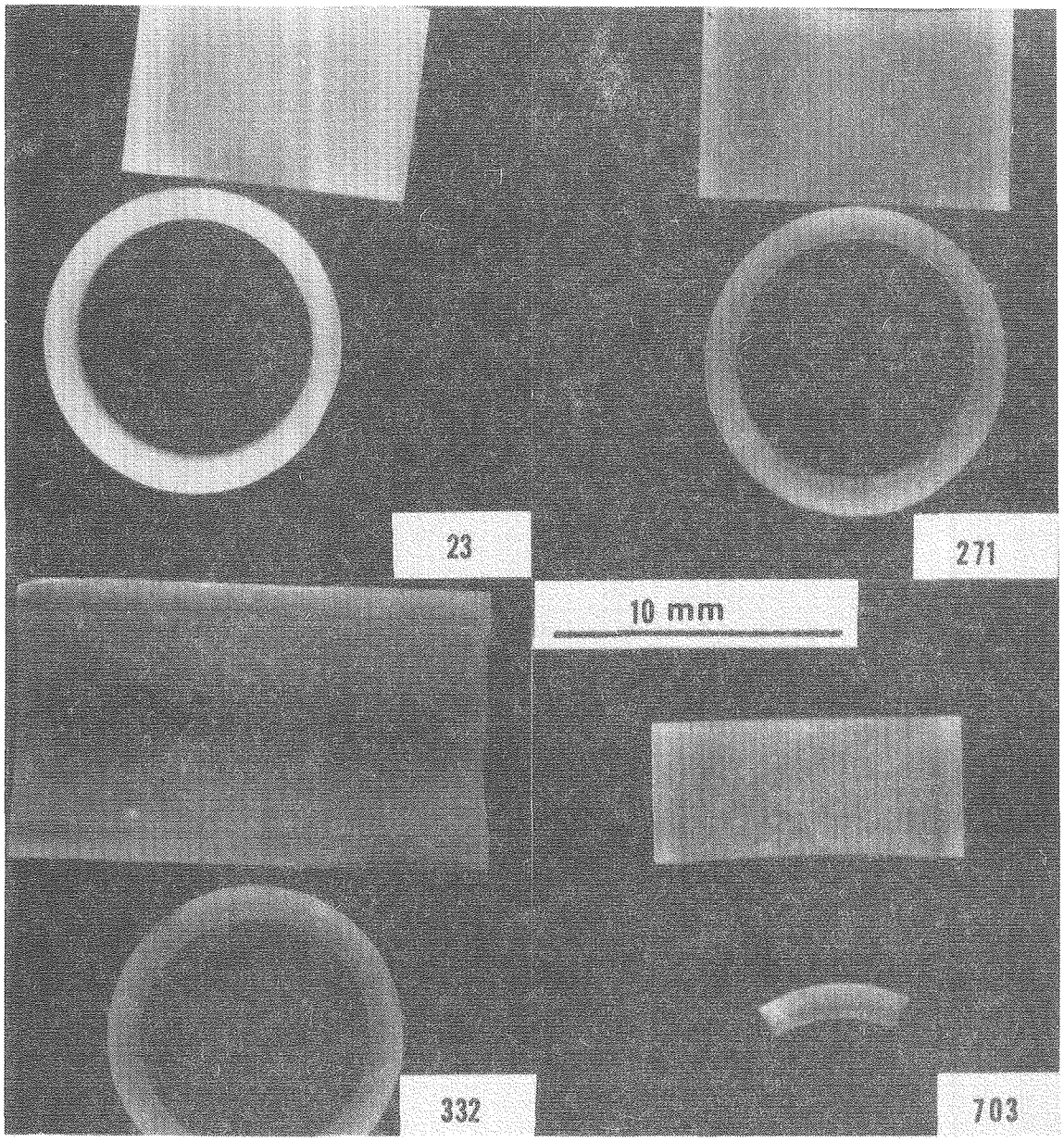

Fig. 1

XBB 804-4133

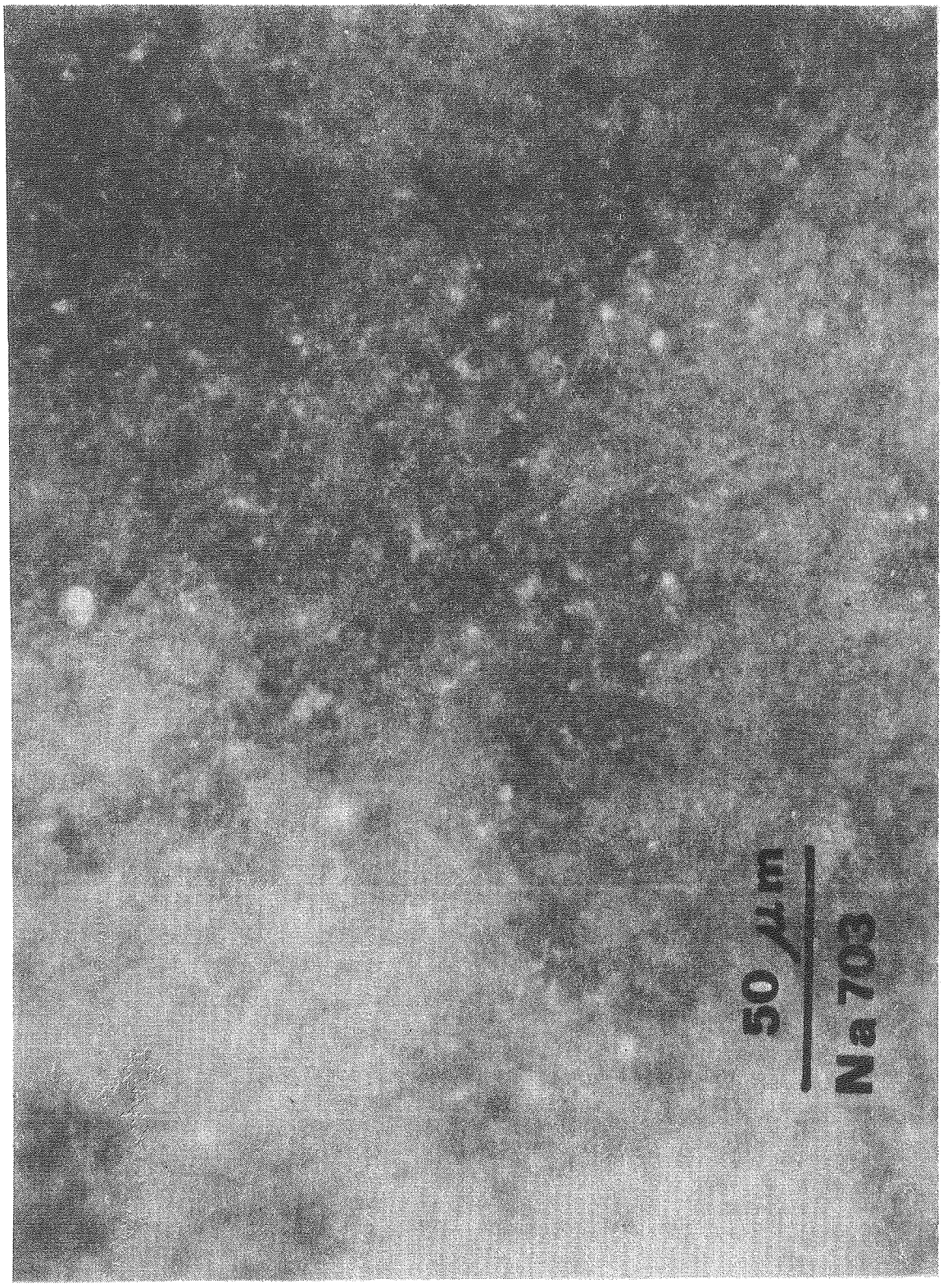

XBB 804-4123

Fig. 2

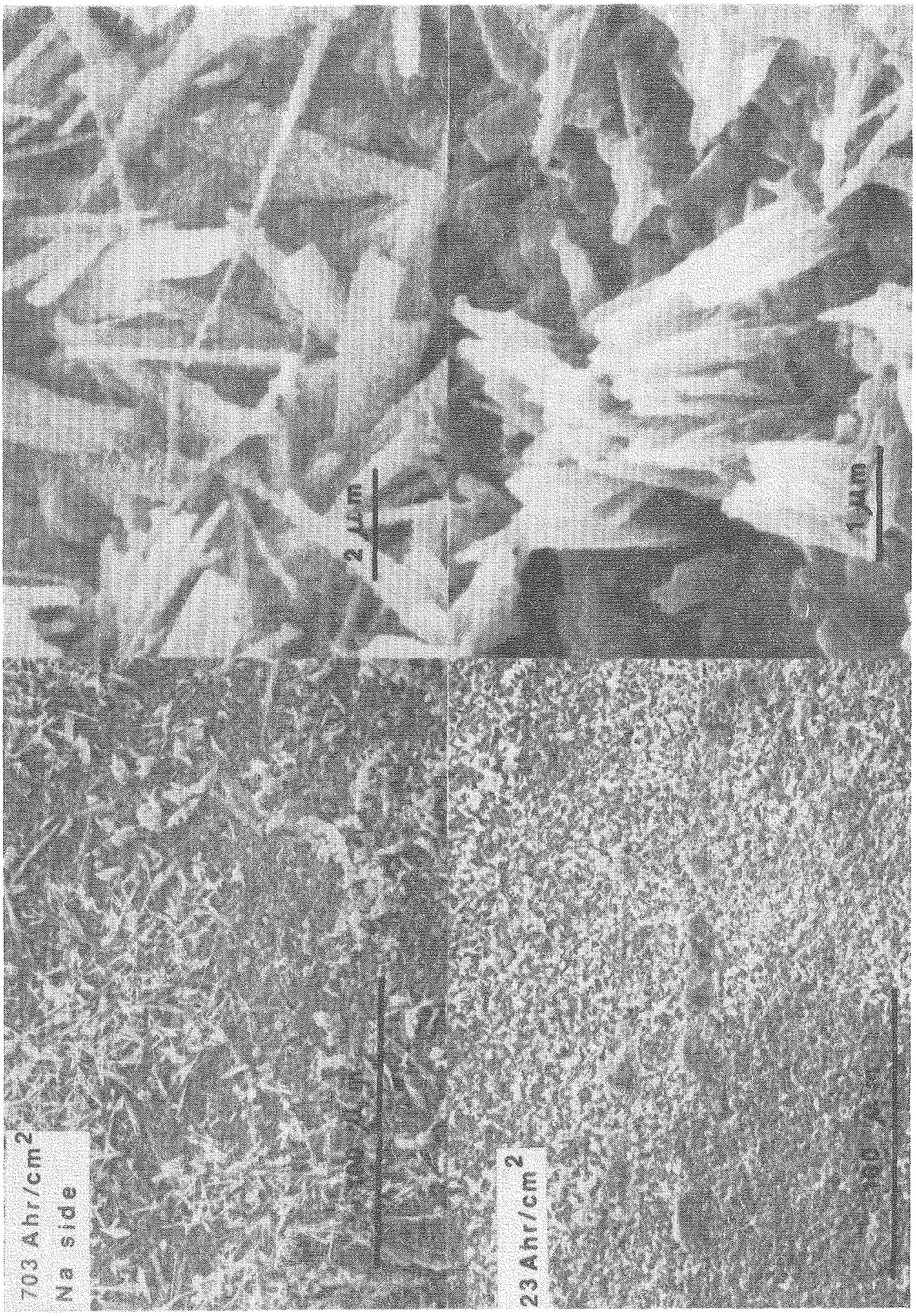

Fig. 3

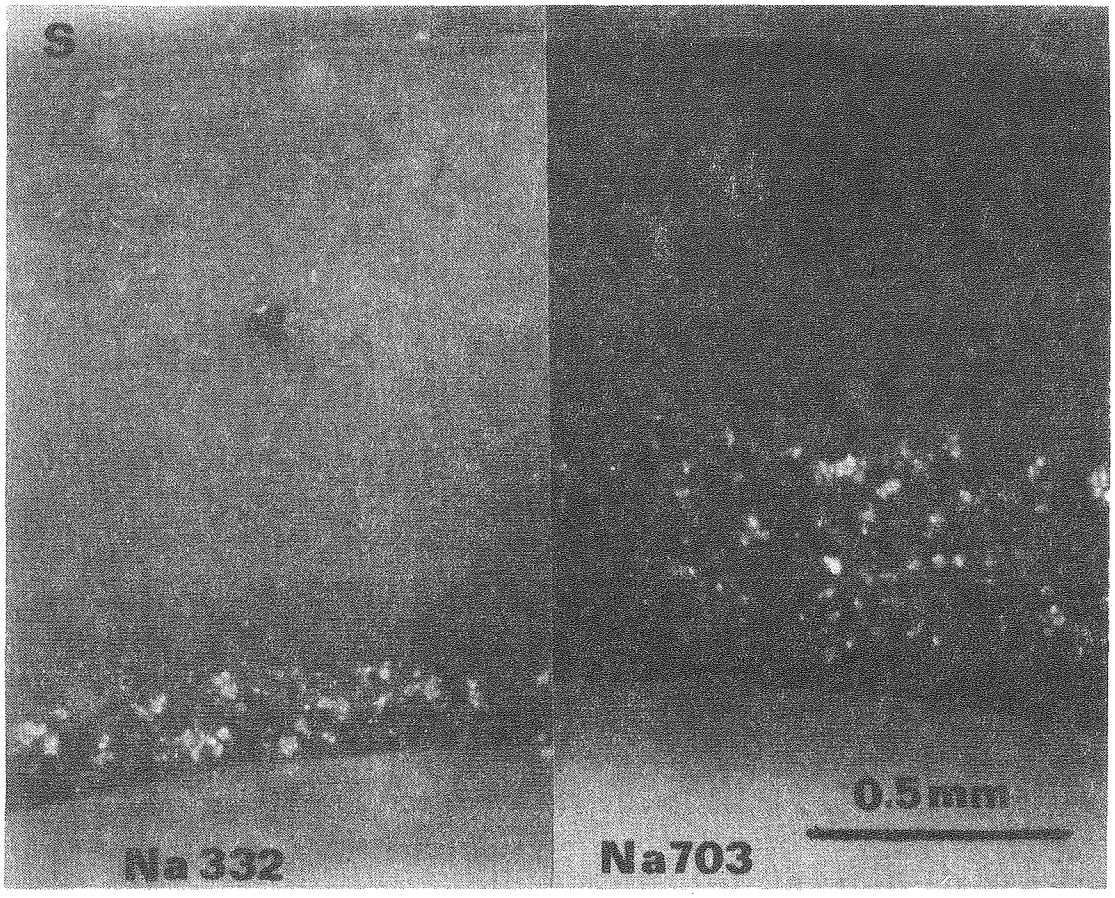

Fig. 4

XBB 804-4119

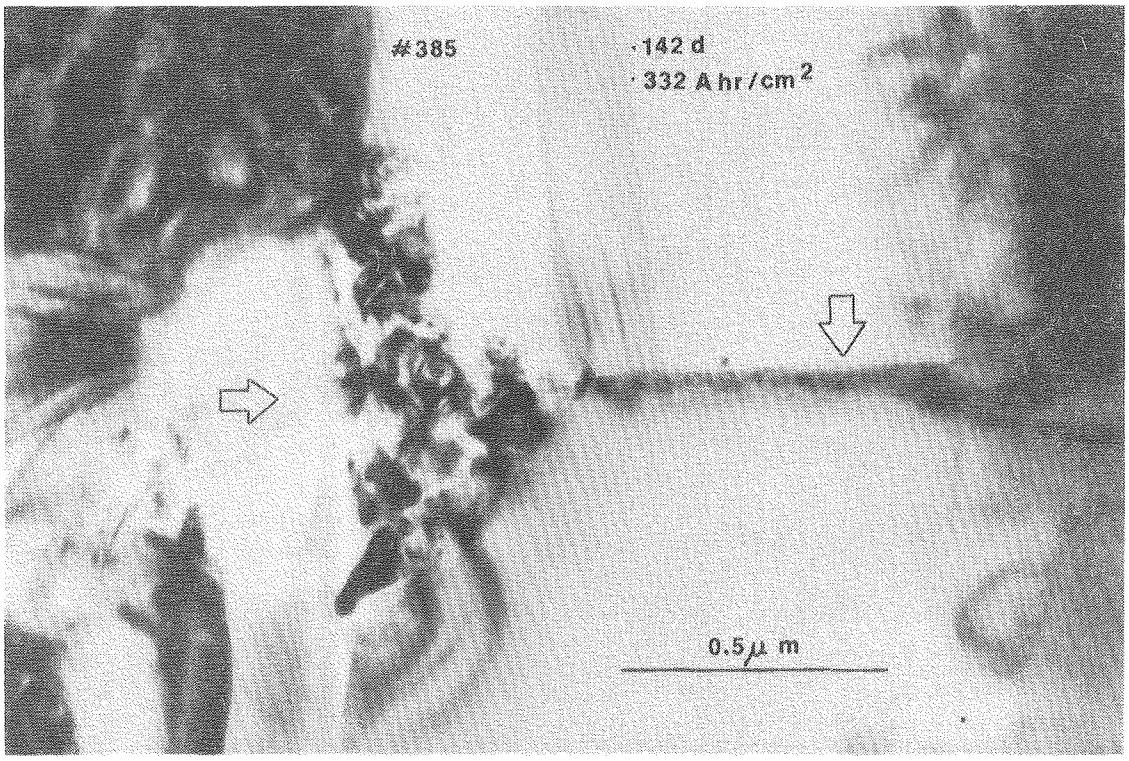

Fig. 5a

XBB 803-3889

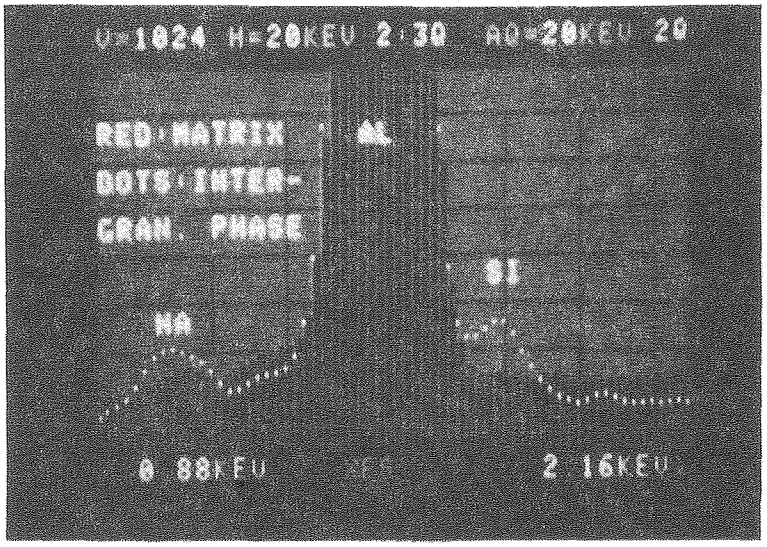

Fig. 5b

CBB 803-3568

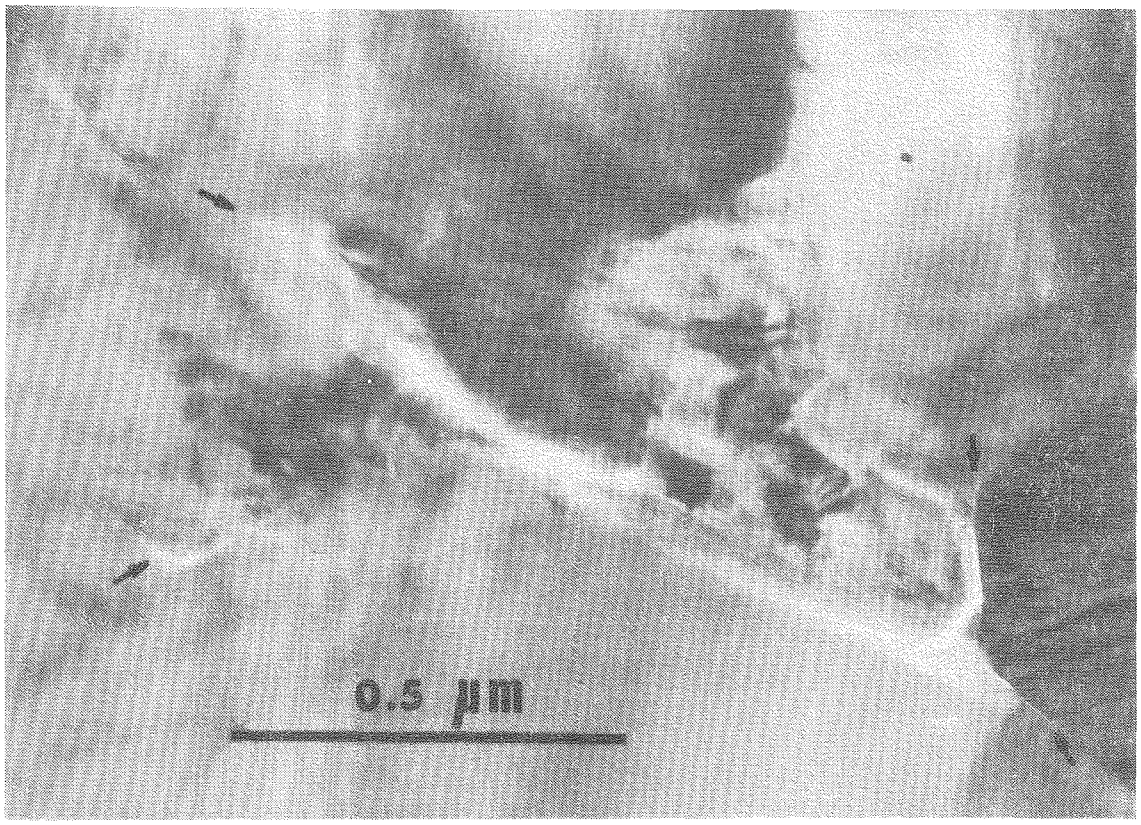

Fig. 6

XBB 806-7055

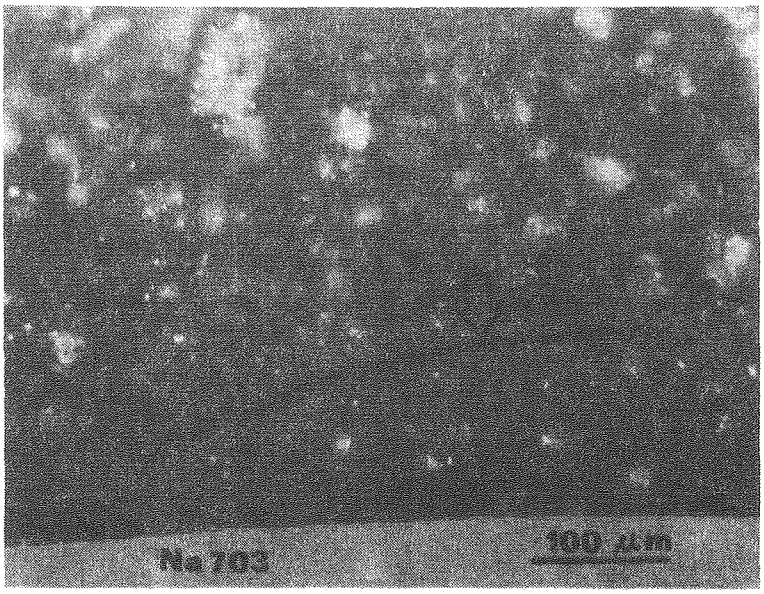

Fig. 7

XBB 804-4120

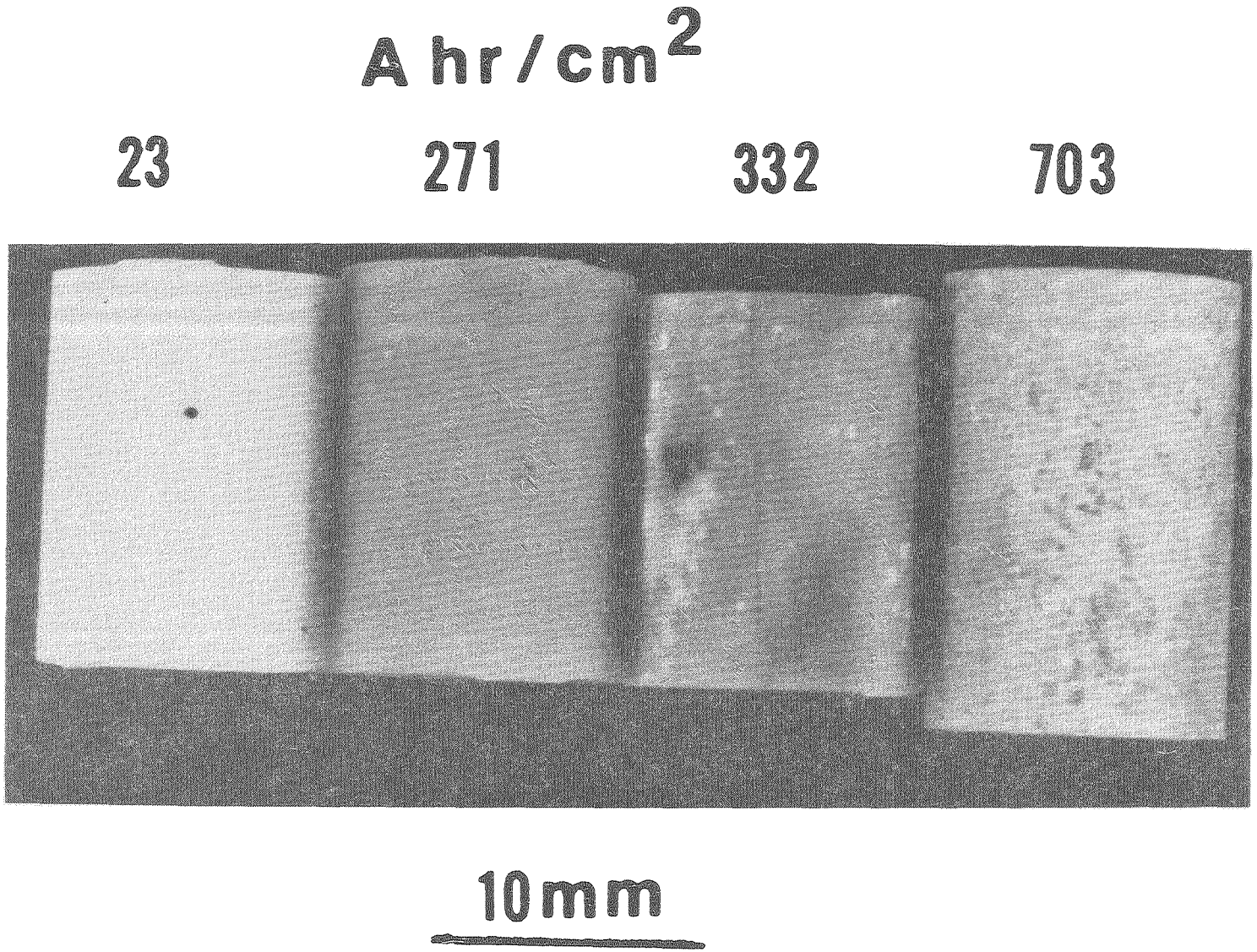

Fig. 8

XBB 804-4114

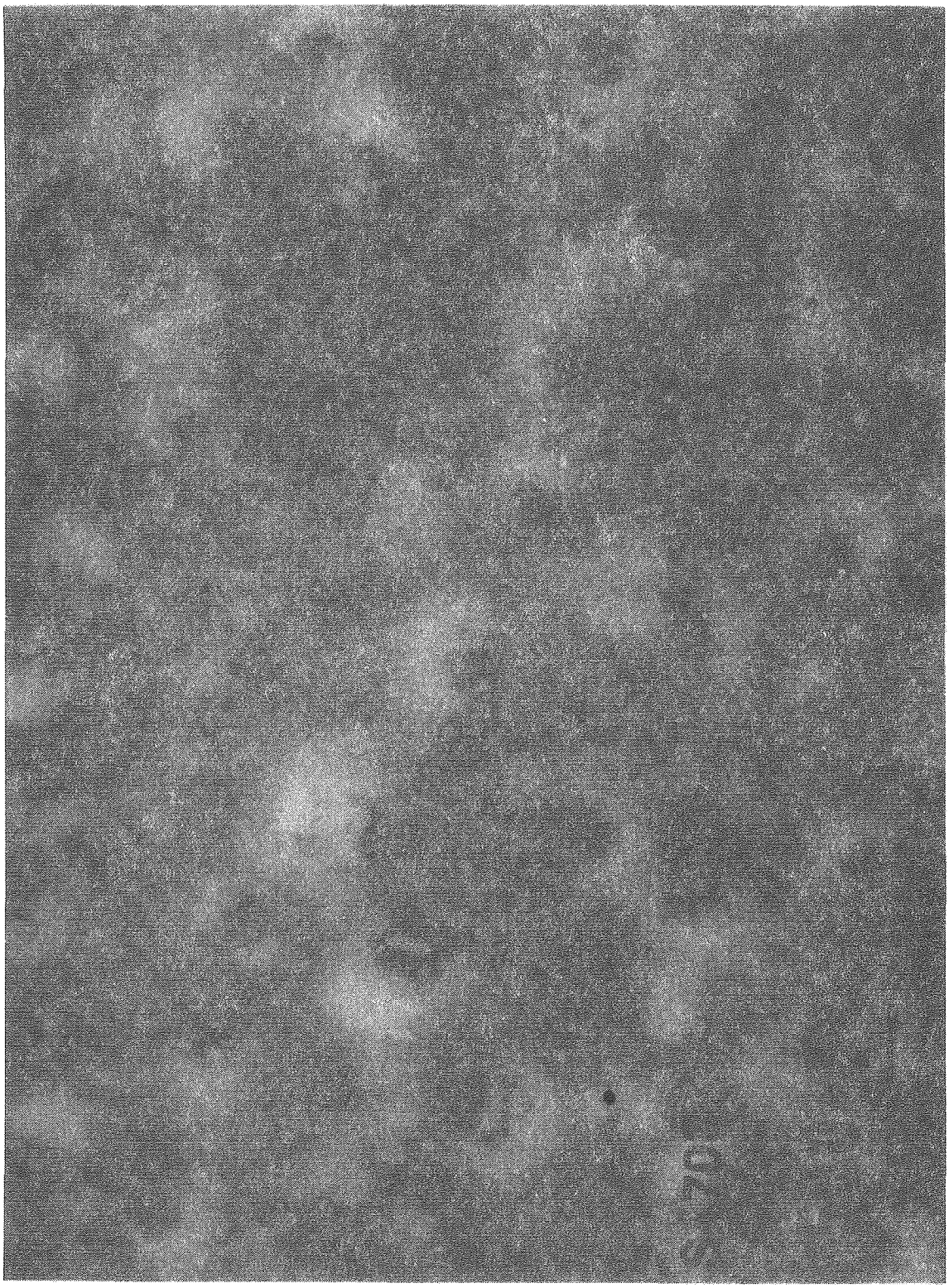

XBB 804-4125

Fig. 9a

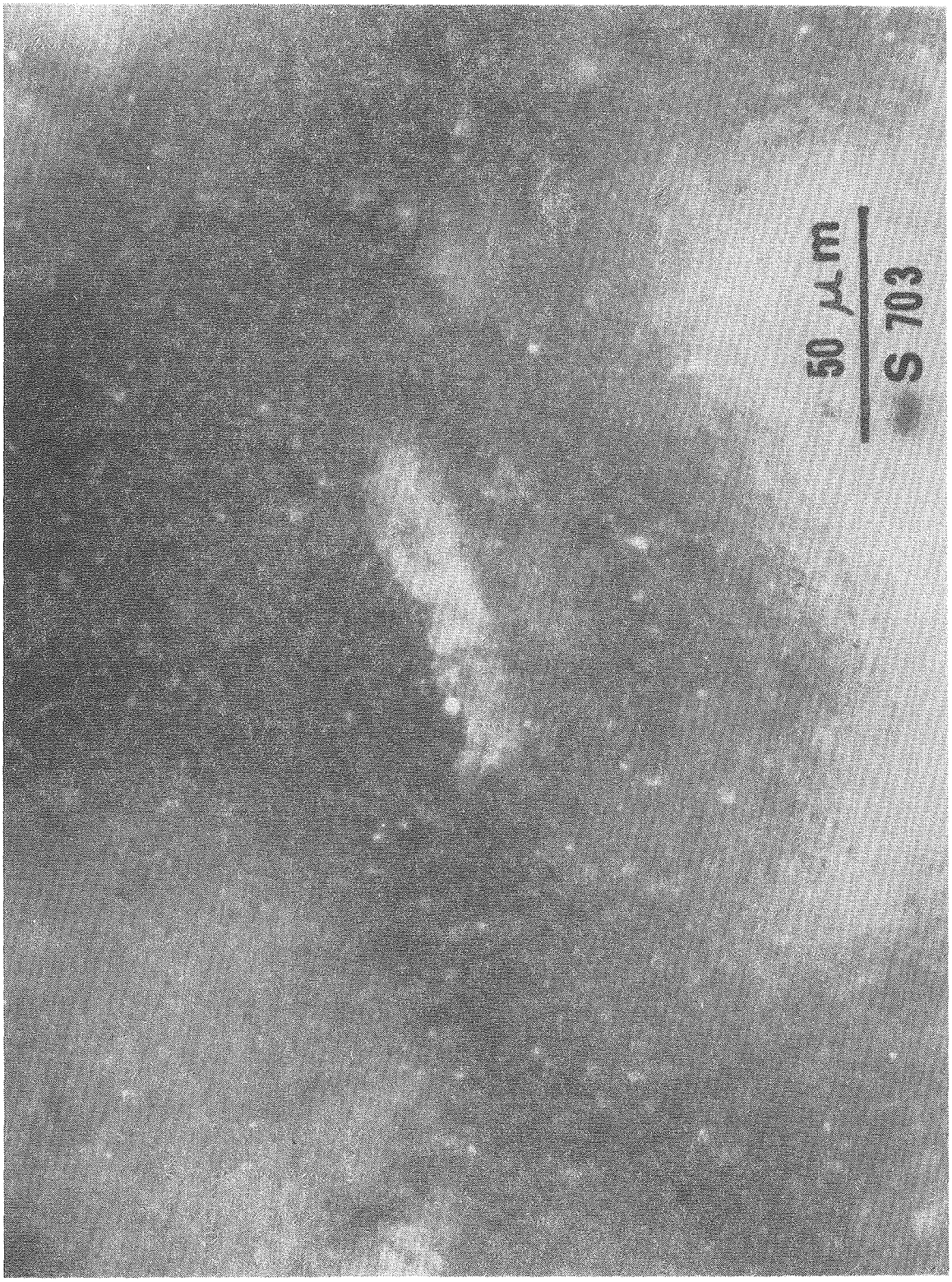

XBB 804-4126

Fig. 9b

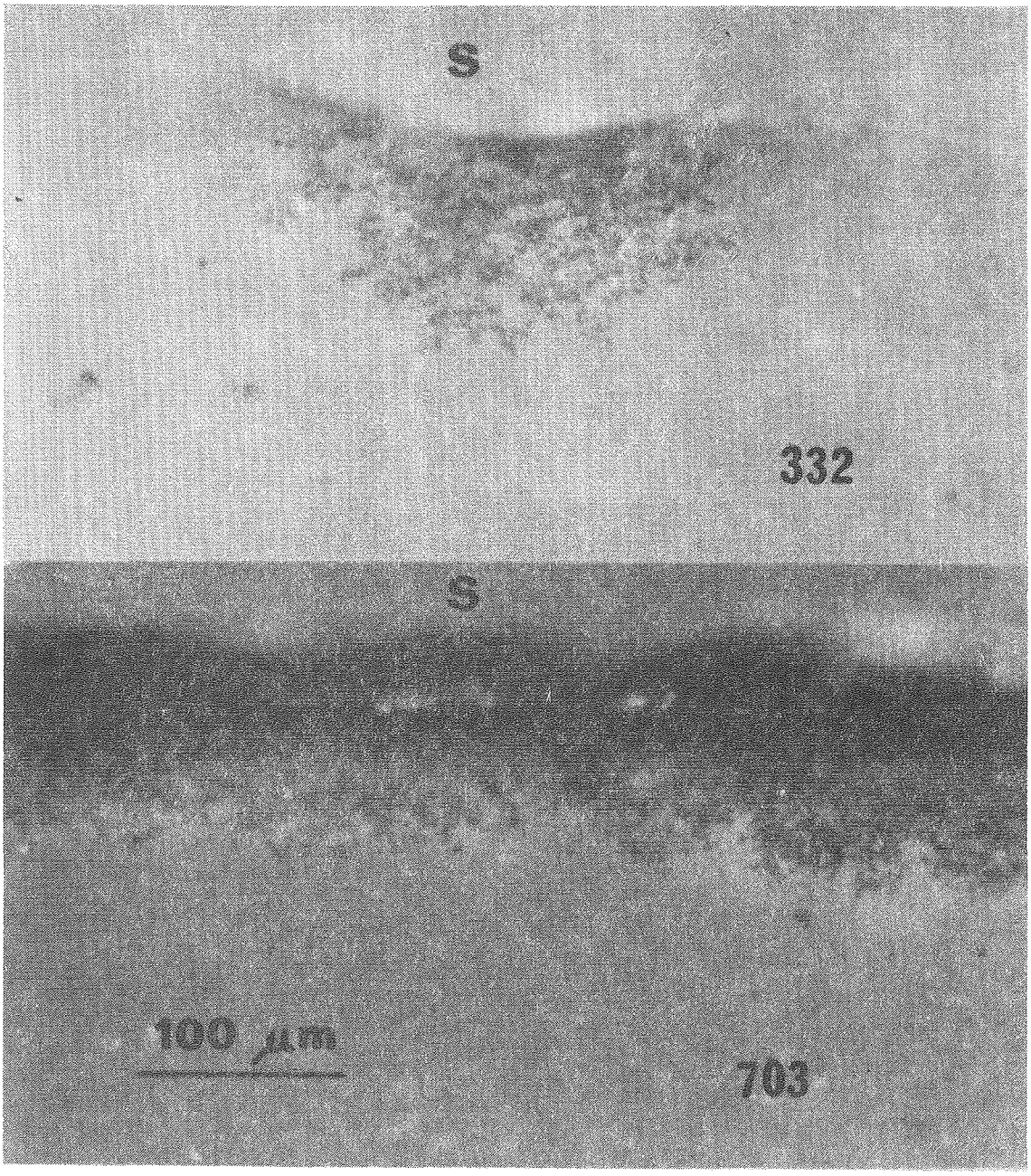

Fig. 10

XBB 804-4128